COMMUNICATIONS IN NUMERICAL METHODS IN ENGINEERING, Vol. 13, 327–336 (1997)

FRACTURE AND DAMAGE ANALYSIS OF A CRACKED BODY BY A NEW BOUNDARY ELEMENT MODEL

Q. H. QIN* AND S. W. YU

Dept. of Eng. Mechanics, Tsinghua University, Beijing, 100084, P. R. China

SUMMARY

Based on the concept of discontinuity displacement, an analytical solution for cracked thin plates has been derived in which displacements and stresses in a solid can be expressed by the linear distributed discontinuity displacements on the whole boundary. By way of the potential variational principle and the analytical solution newly developed, a boundary element model for 2D multiple crack problems has been presented and applied to fracture and damage analysis of thin plates with many cracks. Two numerical examples are considered to illustrate applications of the proposed element model. © 1997 by John Wiley & Sons, Ltd.

Commun. numer. meth. engng., **13**, 327–336 (1997).
No. of Figures: 5 No. of Tables: 2 No. of References: 11

KEY WORDS crack; boundary element method; effective mechanical properties; discontinuity displacement method; variational principle; stress intensity factor

1. INTRODUCTION

The numerical models of brittle materials with many cracks are of considerable interest to engineers and have consequently received a great deal of attention.[1] Current research into the development of efficient methods for crack problems to evaluate the fracture behaviour has mostly concentrated on the self-consistent method,[2] differential scheme,[3] Mori–Tanaka method,[4] generalized self-consistent method,[5] dislocation method,[6] displacement discontinuity method,[7,8] finite element method (FEM)[1,9] and boundary element method.[10] Of all the methods, FEM and the boundary element methods are the most versatile, but the main disadvantage of FEM is that a domain discretization is required to perform the analysis. Moreover, in some cases, it results in both an inaccurate and expensive technique, especially in solving crack problems. On the other hand, the boundary element method involves only discretization of the boundary of the structure due to the governing differential equation being satisfied exactly inside the domain leading to a relatively smaller system size with sufficient accuracy. This is an important advantage over 'domain' type solutions, such as FEM or the finite difference method.

This study presents a new formulation about the displacement discontinuity method, which is the extension of Crouch's solution from a constant element to a linear element.[7] The formulation is based on the analytical solution to the problem of a linearly varying discontinuity in displacement over a finite line segment in the x, y plane of an infinite elastics solid developed in Section 2. Using the solution, the stress intensity factor (SIF) and effective material properties of

* Correspondence to: Q. H. Qin, Dept. of Eng. Mechanics, Tsinghua University, Beijing, 100084, P. R. China

CCC 1069–8299/97/050327–10$17·50

Received 19 December 1995
Revised 8 July 1996

a cracked solid are obtained. It forms the basis of understanding of the statistics of microcracks in composite materials.

2. STATEMENT OF THE PROBLEM

2.1. *Basic relations*

Consider a two-dimensional elastic body inside of which there exist a number of microcracks with arbitrary orientations and sizes. Throughout this paper, indices i and j have values in the range $\{1,2\}$ and the summation convention is used over repeated indices. The problem may then be stated as:

$$\sigma_{ij,j} = 0 \qquad \text{in } \Omega \tag{1}$$

$$p_i = \sigma_{ij,j} n_j = \bar{T}_i \qquad \text{on } \Gamma_\sigma \tag{2}$$

$$u_i = \bar{u}_i \qquad \text{on } \Gamma_u \tag{3}$$

$$p_i\,|_{\Gamma_*^+} = -p_i\,|_{\Gamma_*^-} \qquad \text{on } \Gamma_*^\sigma \tag{4}$$

$$\hat{u}_i = u_i\,|_{\Gamma_*^+} - u_i\,|_{\Gamma_*^-} \qquad \text{on } \Gamma_*^u \tag{5}$$

where σ_{ij} denotes the stress tensor, n_i is the unit normal to the boundary $\partial\Omega(\partial\Omega = \Gamma_\sigma \cup \Gamma_u \cup \Gamma_*)$, Γ_σ and Γ_u are the boundaries on which the stresses and displacements are prescribed, respectively, $\Gamma* = \Gamma_*^\sigma \cup \Gamma_*^u$ designates the crack surface, u_i is the displacement vector, the over bar denotes the prescribed variable, and Γ_*^+ and Γ_*^- are shown in Figure 1.

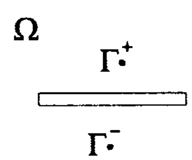

Figure 1. The configuration of the solid

2.2. *Boundary element formulation*

For the boundary value problem (1)–(5), the standard boundary integral equations can be obtained by using the principle of potential energy,[8]

$$\delta\Pi(\hat{u}_i) = \frac{1}{2}\int_{\partial\Omega} (\delta R_i \hat{u}_{i,s} + R_i \delta\hat{u}_{i,s})\, \mathrm{d}s - \int_{\Gamma_\sigma} \bar{T}_i \delta\hat{u}_i\, \mathrm{d}s = 0 \tag{6}$$

in which δ denotes a variational symbol, a comma followed by an argument stands for differentiation with respect to the argument, s is the arc variable on the boundary, and

$$R_i = \int \sigma_{ij} n_j\, \mathrm{d}s \tag{7}$$

The analytical solution of (6) is not, in general, possible, and therefore a numerical procedure must be used to solve the equation. As in the conventional boundary element method, the

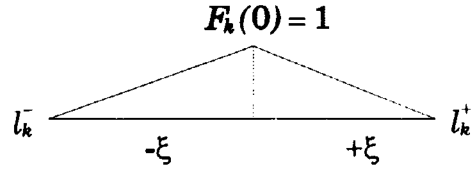

Figure 2. The definitions for l_k^-, l_k^+ and $F_k(s)$

boundary integral equation (6) is approximated by using the BE technique with N boundary elements, and the unknown variable, $\hat{u}_i$, in each element is interpolated by some shape functions. As an illustration, consider a particular crack line, say the jth crack, in the region Ω, and then divide the line into M_j straight segments, joined end to end. The displacement discontinuity ($\hat{\mathbf{u}} = \{\hat{u}_1, \hat{u}_2\}$) may then be approximated by the sum of elemental displacement discontinuities

$$\hat{\mathbf{u}}(s) = \sum_{k=1}^{M_j} \hat{\mathbf{u}}^{(k)} F_k(s) \tag{8}$$

where $\hat{\mathbf{u}}^{(k)}$ is the vector of discontinuity displacements at node k, and $F_k(s)$ is a global shape function associated with the kth node. F_k is zero-valued over the whole mesh except within two elements connected to the kth node (see Figure 2). Over these two elements $F_k(s)$ is assumed to be linear, i.e.

$$F_k(s) = \begin{cases} \dfrac{l_k^- + s}{l_k^-} & \text{if} \quad s \leqslant 0 \\ \dfrac{l_k^+ - s}{l_k^+} & \text{if} \quad s \geqslant 0 \end{cases} \tag{9}$$

As was done in Reference 7, the resultant force $R_i(x, y)$, displacement $u_i(x, y)$ and stress $\sigma_{ij}(x, y)$ can be deduced from a particular function, say $\phi_m(x, y)$. The function is determined by

$$4\pi(1-\nu)\frac{\partial \phi_m(x, y)}{\partial y} = \frac{\partial}{\partial y}\int_{l_i^-}^{l_i^+} \hat{u}_m(\xi)\ln[(x-\xi)^2 + y^2]\,\mathrm{d}\xi \tag{10}$$

Substituting (8) into (10) and noting that

$$\begin{aligned} &\int \xi \ln[(x-\xi)^2 + y^2]\,\mathrm{d}\xi = \int\left(\frac{1}{2}\ln z\,\mathrm{d}z + x\ln z\,\mathrm{d}\xi\right) \\ &\frac{1}{2}\int \ln[(x-\xi)^2 + y^2]\,\mathrm{d}\xi = y\tan^{-1}\left(\frac{y}{x-\xi}\right) - \tfrac{1}{2}(x-\xi)\ln[(x-\xi)^2 + y^2] - \xi \end{aligned} \tag{11}$$

with

$$z = (x-\xi)^2 + y^2$$

we have

$$
\begin{aligned}
\phi_m(x,y) = {} & \frac{(l_i^- + x)\hat{u}_m}{4\pi(1-\nu)l_i^-}\left[-y\tan^{-1}\left(\frac{y}{x+l_i^-}\right) + y\tan^{-1}\left(\frac{y}{x}\right) - l_i^-\right. \\
& \left. + (x+l_i^-)\ln\sqrt{(x+l_i^-)^2+y^2} - x\ln\sqrt{x^2+y^2}\right] \\
& + \frac{(l_i^+ - x)\hat{u}_m}{4\pi(1-\nu)l_i^+}\left[y\tan^{-1}\left(\frac{y}{x-l_i^+}\right) - y\tan^{-1}\left(\frac{y}{x}\right) - l_i^+\right. \\
& \left. - (x-l_i^+)\ln\sqrt{(x-l_i^+)^2+y^2} + x\ln\sqrt{x^2+y^2}\right] \\
& + \frac{\hat{u}_m}{16\pi(1-\nu)l_i^-}\{(x^2+y^2)\ln(x^2+y^2) + 2xl_i^- + (l_i^-)^2 \\
& - [(x^2+l_i^-)^2+y^2]\ln[(x^2+l_i^-)^2+y^2]\} \\
& - \frac{\hat{u}_m}{16\pi(1-\nu)l_i^+}\{-(x^2+y^2)\ln(x^2+y^2) + 2xl_i^+ - (l_i^+)^2 \\
& + [(x^2-l_i^+)^2+y^2]\ln[(x^2-l_i^-)^2+y^2]\}
\end{aligned}
\tag{12}
$$

Note that the formulation developed above is based on the analytical solution to the problem of a linear displacement discontinuity over an arbitrarily oriented, finite line segment in an infinite solid. In applications, it proves useful to express this solution in the global co-ordinate system, which can be done with the aid of a simple co-ordinate transformation. Denoting the local and global Cartesian co-ordinate systems by (x, y) and (X, Y) illustrated in Figure 3, the local co-ordinates (x, y) are related to the global co-ordinates (X, Y) by

$$
\begin{aligned}
x &= (X-c_x)\cos\theta + (Y-c_y)\sin\theta \\
y &= -(X-c_x)\sin\theta + (Y-c_y)\cos\theta
\end{aligned}
\tag{13}
$$

where c_x, c_y and θ are defined in Figure 3.

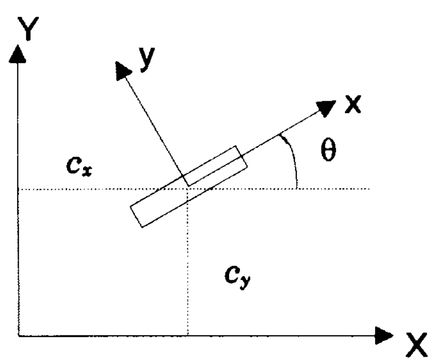

Figure 3. The local and global co-ordinate systems

Correspondingly, the displacements and stresses in two co-ordinate systems are related by

$$\begin{aligned}
u_X &= u_x \cos\theta - u_y \sin\theta \\
u_Y &= u_x \sin\theta + u_y \cos\theta \\
\sigma_{XX} &= \sigma_{xx} \cos^2\theta - 2\sigma_{xy} \cos\theta \sin\theta + \sigma_{yy} \sin^2\theta \\
\sigma_{XY} &= (\sigma_{xx} - \sigma_{yy})\cos\theta \sin\theta + \sigma_{xy}(\cos^2\theta - \sin^2\theta) \\
\sigma_{YY} &= \sigma_{xx} \sin^2\theta + 2\sigma_{xy} \cos\theta \sin\theta + \sigma_{yy} \cos^2\theta
\end{aligned} \tag{14}$$

Substituting (8) into (6) and noting (14), one obtains

$$K^{IJ} D^J = F^I \tag{15}$$

where $D^J = \{\hat{u}_X^J \hat{u}_Y^J\}^T$ is the nodal displacement discontinuity vector in the global co-ordinate system, E_J^- and E_J^+ are two elements connected to the Jth node: E_J^- is to the left and E_J^+ to the right, l_j^- and l_j^+ stand for their length, and

$$\begin{aligned}
K^{IJ} &= H^T \hat{K}_{IJ} H \\
H &= \begin{bmatrix} \cos\theta & \sin\theta \\ -\sin\theta & \cos\theta \end{bmatrix} \\
\hat{K}_{IJ} &= \frac{1}{l_j^-}\int_{E_J^-} \begin{bmatrix} C_{xx}^I & C_{xy}^I \\ C_{yx}^I & C_{yy}^I \end{bmatrix} \mathrm{d}s - \frac{1}{l_j^+}\int_{E_J^+} \begin{bmatrix} C_{xx}^I & C_{xy}^I \\ C_{yx}^I & C_{yy}^I \end{bmatrix} \mathrm{d}s \\
F^I &= H^T \int_{E_I^- \cup E_I^+} \bar{T}(s) F_I(s) \mathrm{d}s \\
C_{xx}^I &= -2G(\phi_{,x}^I + y\phi_{,xy}^I), \quad C_{xy}^I = -2Gy\phi_{,yy}^I \\
C_{yx}^I &= C_{xy}^I, \quad C_{yy}^I = 2G(y\phi_{,xy}^I - \phi_{,x}^I)
\end{aligned} \tag{16}$$

with

$$\phi_m^I(x, y) = \hat{u}_m^I \phi^I(x, y) \quad (I \text{ not summed})$$

Solving (15), the displacement discontinuities of the whole structure are obtained and then other field variables can be evaluated from $\hat{u}_i$.

3. OVERALL MODULI AND STRESS INTENSITY FACTORS

3.1. Overall moduli

The effective mechanical properties due to the presence of microcracks are discussed in this subsection. Consider a rectangular element with area A, bounded by the exterior Γ and weakened by many cracks with lengths l_k ($k = 1, \ldots, N$; see Figure 4). The strain–stress relation for the cracked element can be written as

$$\bar{\varepsilon}_{ij} = s_{ijkl}^0 \bar{\sigma}_{kl} + \frac{1}{2A}\sum_{k=1}^{N} \int_{l_k} (b'_{ki} n'_j + b'_{kj} n'_i)\, \mathrm{d}l = (s_{ijkl}^0 + s_{ijkl}^*)\bar{\sigma}_{kl} \tag{17}$$

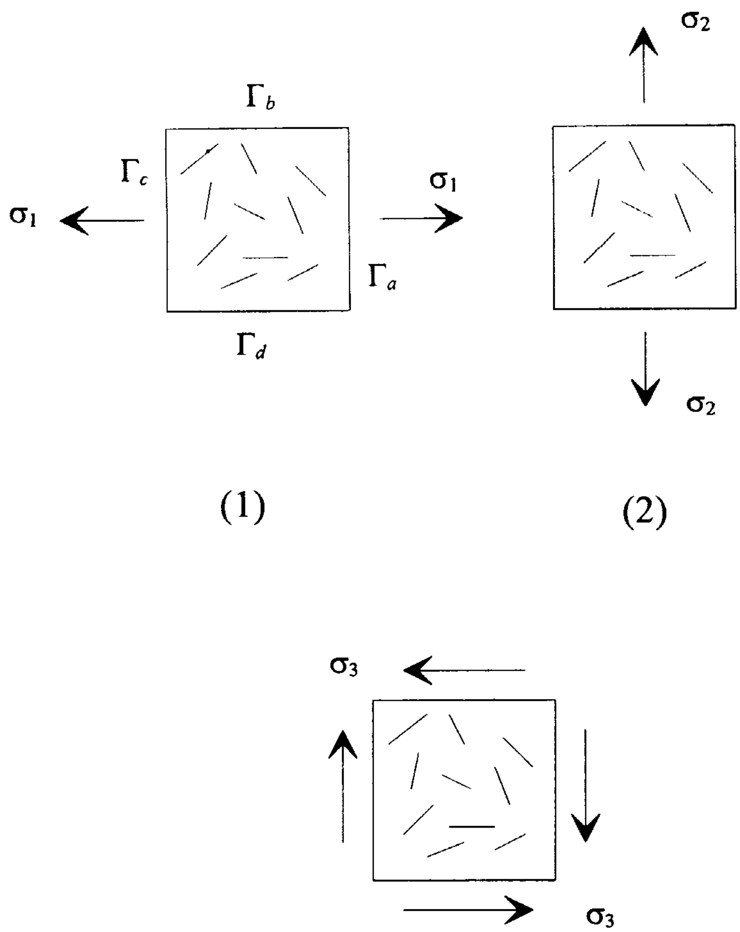

Figure 4. Load configuration of the cracked body

where s^0_{ijkm} is the compliance tensor of the undamaged solid, and b'_{ki} and n'_i are, respectively, the displacement discontinuity and the normal to the kth crack faces, $\bar{\varepsilon}_{ij}$ and $\bar{\sigma}_{ij}$ the average strain and stress tensors over the area A, and the prime refers to the co-ordinate system local to the crack in which the x_1-axis coincides with the crack line. Consider further, following three loading cases (see Figure 4), the related components of the inelastic compliance, given by

$$\begin{Bmatrix} S_{11} \\ S_{21} \\ S_{61} \end{Bmatrix} = \begin{Bmatrix} s_{1111} \\ s_{2211} \\ s_{1211} \end{Bmatrix} = \frac{1}{\sigma_1} \begin{Bmatrix} \varepsilon_{11} \\ \varepsilon_{22} \\ 2\varepsilon_{12} \end{Bmatrix}_{\sigma=\sigma_1} \tag{18}$$

for the load case in Figure 5(a),

$$\begin{Bmatrix} S_{22} \\ S_{62} \end{Bmatrix} = \begin{Bmatrix} s_{2222} \\ s_{1222} \end{Bmatrix} = \frac{1}{\sigma_2} \begin{Bmatrix} \varepsilon_{22} \\ 2\varepsilon_{12} \end{Bmatrix}_{\sigma=\sigma_2} \tag{19}$$

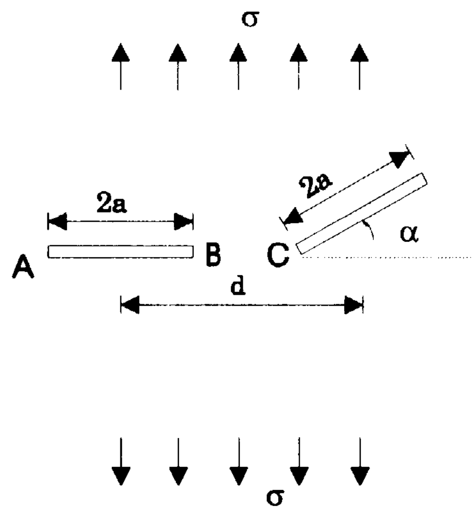

Figure 5. One crack in horizontal and another in inclined position

for Figure 5(b), and

$$S_{66} = s_{1212} = \left.\frac{2\varepsilon_{12}}{\sigma_3}\right|_{\sigma=\sigma_3} \tag{20}$$

for Figure 5(c), in which

$$\varepsilon_{11} = \frac{1}{A}\left[\int_{\Gamma_a} \hat{u}_1 \, \mathrm{d}l - \int_{\Gamma_c} \hat{u}_1 \, \mathrm{d}l\right] \tag{21}$$

$$\varepsilon_{22} = \frac{1}{A}\left[\int_{\Gamma_b} \hat{u}_2 \, \mathrm{d}l - \int_{\Gamma_d} \hat{u}_2 \, \mathrm{d}l\right] \tag{22}$$

$$2\varepsilon_{12} = \frac{1}{A}\left[\int_{\Gamma_d} \hat{u}_1 \, \mathrm{d}l - \int_{\Gamma_b} \hat{u}_1 \, \mathrm{d}l + \int_{\Gamma_c} \hat{u}_2 \, \mathrm{d}l - \int_{\Gamma_a} \hat{u}_2 \, \mathrm{d}l\right] \tag{23}$$

3.2. Stress intensity factors

There are several ways for evaluating the stress intensity factors from the boundary element method, such as extrapolation of displacement discontinuities to the crack tip, the J-integral, the energy approach and the virtual crack extension technique. The last method is used to calculate the stress intensity factors in our study. In this method, the change of δU due to a particular crack extension, say the kth crack, is evaluated by displacing the nodal points within the crack tip element by an incremental distance δl_k. Then the stress intensity factor can be calculated from the strain energy release rate $G_{(k)}$ using the relation

$$G_{(k)} = \frac{\delta U}{\delta l_k} = \bar{A}(K_{I(k)}^2 + K_{II(k)}^2) \tag{24}$$

in which $\bar{A} = (1 - \nu^2)/E$ for plane strain, $\bar{A} = 1/E$ for plane stress, and δU stands for the strain energies before and after the kth crack extension. Therefore, we have

$$G_{(k)} = \frac{\delta U}{\delta l_{(k)}} = -\frac{\delta}{2\delta l_k}\sum_m \int_{l_m} t_j \hat{u}_j \, \mathrm{d}s \approx -\frac{\delta}{2\delta l_k}\sum_m (t_j^{(m)} \hat{u}_j^{(m)} l_m) \tag{25}$$

where t_j is the traction vector. If the load is due to forces outside the crack tip element, we have

$$G_{(k)} = -\frac{1}{2}\sum_m (t_j^{(m)} \delta\hat{u}_j^{(m)} l_m + t_j^{(m)} \hat{u}_j^{(m)} \delta l_m)/\delta l_k \tag{26}$$

K_I may then be evaluated by

$$K^2_{i(k)} = \frac{\delta U_i}{\delta l_k}/\bar{A} \quad (i = I, II) \tag{27}$$

where

$$\begin{aligned} U_I &\approx -\frac{1}{2}\sum_k \sum_{j=1}^{2} t_j^{(k)} \hat{u}_j^{(k)} n_j^{(k)} l_k \\ U_{II} &\approx -\frac{1}{2}\sum_k \sum_{j=1}^{2} t_j^{(k)} \hat{u}_j^{(k)} s_j^{(k)} l_k \end{aligned} \tag{28}$$

4. NUMERICAL EXAMPLES

As an illustration, the proposed element model is applied to two numerical examples. In all the calculations, we take $\Delta l/l = 10^{-4}$ and $\nu = 0{\cdot}3$, and each crack is divided into ten elements.

Example 1: Consider an infinite thin plate weakened by two cracks (one crack in the horizontal position and another in inclined angle α; see Figure 5). The plate is subjected to a far field as shown in Figure 5. In the calculation, we take $d = 1$ and $a = 0{\cdot}45$ and each crack is divided into ten elements. For the problem, it suffices to consider the associated problem in which crack surfaces are subjected to an equivalent load. For example, for a particular crack, say the kth crack, the equivalent loads acting at the crack surfaces are

$$\begin{aligned} t_n &= \sigma \cos \theta \\ t_s &= -\sigma \sin \theta \end{aligned} \tag{29}$$

where t_n and t_s are the tractions in the normal and tangential directions of the crack line, and θ is defined in Figure 3. In this case the displacements and stresses at infinity are zero and we need not consider the boundary at infinity.

Table I gives the variation of $\beta_i = \mathrm{K}_i/\sigma\sqrt{(\pi a)}$, $i = IA, IIA, IB, IIB, IC, IIC$, with the angle α, and compares with the results in Reference 11. It can be seen from the Tables that, for a relatively small number of elements, the results obtained are in good agreement with those given in Reference 11.

Table I. The coefficients β_j versus angle α in example 1

	α	β_{IA}	β_{IIA}	β_{IB}	β_{IIB}	β_{IC}	β_{IIC}
Present	0°	1·1195	0	1·4732	0	1·4732	0
Ref. [11]	0°	1·1195	0	1·4732	0	1·4732	0
Present	30°	1·0942	−0·0483	1·3023	−0·0479	1·0358	0·5538
Ref. [11]	30°	1·0939	−0·0544	1·2933	−0·0522	1·0260	0·5501
Present	60°	1·0258	−0·0123	1·0762	−0·0029	0·3210	0·5322
Ref. [11]	60°	1·0300	−0·0116	1·0753	−0·0035	0·3133	0·5149
Present	90°	1·0032	0	1·0059	0	0·0375	0·0142
Ref. [11]	90°	1·0040	0	1·0071	0	0·0305	0·0133

Table II. $\bar{S}_{11}$ and $\bar{S}_{22}$ versus angle α

α	0°	30°	60°	90°
$\bar{S}_{11}(10^{-5})$	9·100	9·082	9·061	9·045
$\bar{S}_{22}(10^{-5})$	9·018	9·024	9·032	9·044

Example 2: Consider again the two-crack solid in example 1, but with the solution domain taken to be a square with side length = 20. In the calculation, the boundary of the square is modelled by 40 elements and each crack is divided into ten elements. Table II displays the variation of predicted $\bar{S}_{11}$ and $\bar{S}_{22}$ with angle α. The results seem to be reasonable. However, there are no reference values of the effective compliance for this example.

5. CONCLUSIONS

A new boundary element model and a computer program for analysing plane problem with many cracks have been developed in the paper. In this method, the displacement discontinuity (i.e. the jump displacement across crack faces for cracks, the displacement for external boundary) is taken as the basic unknown variable. Using Crouch's method,[7] we obtain an analytical solution for the plane problem of a linearly varying displacement discontinuity over a finite line segment in an infinite elastic solid. With the solution, the SIF and overall moduli of a cracked body are obtained. The formulation can be applied to both the infinite domain (example 1) and the finite domain (example 2). It should be noted that the formulation is only valid for equal length elements within each crack. However, the element length in one crack may be different from that in another crack.

REFERENCES

1. J. Argyris, I. St. Doltsinis, M. Eggers and R. Handel, 'Studies on ceramic coatings: Deduction of mechanical and thermal properties from the microstructure of the material', *Comput. Methods Appl. Mech. Eng.*, **111**, 203–234 (1994).
2. B. Budiansky and R. J. O'Connell, 'Elastic moduli of a cracked solid', *Int. J. Solids Struct.*, **12**, 81–97 (1976).
3. Z. Hashin, 'The differential scheme and its application to cracked bodies', *J. Mech. Phys. Solids*, **36**, 719–734 (1988).
4. T. Chen, G. J. Dvorak and Y. Benveniste, 'Mori-Tanaka estimates of the overall elastic moduli of certain composite materials', *J. Appl. Mech.*, **59**, 539–546 (1992).

5. J. Aboudi and Y. Benveniste, 'The effective moduli of cracked bodies in plane deformation', *Eng. Fract. Mech.*, **26**, 171–184 (1987).
6. K. Y. Lam, W. Cao and T. Zhuang, 'Interaction between microcracks and a main crack in a semi-infinite medium', *Eng. Fract. Mech.*, **44**, 753–761 (1993).
7. S. L. Crouch, 'Solution of plane elasticity problems by the displacement discontinuity method', *Int. J. Numer. Methods Eng.*, **10**, 135–153 (1976).
8. H. P. Yin and A. Ehrlacher, 'Variational approach of displacement discontinuity method and application to crack problems', *Int. J. Fract.*, **63**, 135–153 (1993).
9. M. H. Aliabadi and D. P. Rooke, *Numerical Fracture Mechanics*, Kluwer Academic Pub., 1992.
10. S. L. Crouch and A. M. Starfield, *Boundary Element Methods in Solid Mechanics*, George Allen & Unwin Ltd., 1983.
11. Y. Z. Chen, 'New Fredholm integral equation for multiple crack problem in plane elasticity and antiplane elasticity', *Int. J. Fract.*, **64**, 63–77 (1993).